

Post-Earthquake Fire Performance of Buildings: Summary of a Large-Scale Experiment and Conceptual Framework for Integrated Performance-Based Seismic and Fire Design

*Brian J. Meacham**, Department of Fire Protection Engineering, Worcester Polytechnic Institute, 100 Institute Road, Worcester, MA 01609, USA

Received: 8 May 2015/**Accepted:** 17 July 2015

Abstract. A full-scale, five-story reinforced concrete building test specimen was erected on the large outdoor high performance shake table at the University of California, San Diego, and outfitted with various nonstructural components and systems. The specimen was subjected to a series of thirteen earthquake motions: seven with base-isolation and six with fixed-base (FB), with peak accelerations up to 0.8 g and peak inter-story drift ratios of up to about 6% reached during the largest FB motion. Damage to the structure following the largest motion included densely concentrated cracking in the slabs around columns resulting in punching shear failure, concrete spalling at the base of columns and the ends of beams where the large rotations occurred, as well as fractured and yielded longitudinal rebar in the Floor 2 and Floor 3 frame beams. Nonstructural component and system damage included loss of stair connections at Floors 3 and 4 due to weld fractures, loss of elevator function due to damaged doors on Floors 2 and 3, widespread damage to gypsum wallboard and joints, with about a 900% increase in effective leakage area measured in one compartment, varying degrees of damage to ceiling system based on type, including loss of 20% of ceiling tiles on the Floor 1, extensive damage to the balloon-framed façade system which enclosed Floors 1, 2 and 3, and displacement of unanchored contents. Following the motion tests, designated areas on Floor 3 were subjected to fires ranging in size from 500 kW to 2000 kW. Many fire protection systems, such as the sprinkler system and most firestop systems performed well. However, loss of compartmentation due to ground motions provided means for smoke spread, and loss of the stairs and the elevator rendered the means of egress unusable. Post experiment analysis illustrates how such damage could impact occupant life safety and emergency response during fires in earthquake-damaged buildings, and how the understanding of expected earthquake damage could be integrated into a risk-informed performance-based approach to building fire safety design in earthquake prone areas.

Keywords: Earthquake performance, Post-earthquake fire performance, Full-scale experiments, Design guidance

* Correspondence should be addressed to: Brian J. Meacham, E-mail: bmeacham@wpi.edu



1. Introduction

In recent decades, earthquakes have resulted in significant damage to key building fire and life safety components, both passive and active, including façade components (glazing, curtain wall systems, and other exterior systems), interior partitions, ceiling systems, access and egress components (doors, stairs, elevators), ventilation (including smoke control) systems, detection and alarm systems, suppression systems, lighting systems, and electrical power systems [1–13]. In the Northridge, CA, USA and Hyogoken-Nanbu, Japan, earthquakes, numerous building fire protection systems experienced significant damage [3–5, 7–9], including up to 40% of the sprinkler systems and 30% of the fire doors [8, 9]. These data are consistent with damage reported from the 1993 Kushiro-oki earthquake and the 1994 Sanriku-haruka-oki earthquake as well [9].

Access and egress components have also been shown to perform poorly in some earthquakes. In the 22 February 2011 Christchurch Earthquake, precast stair units collapsed in at least four multi-story buildings and were severely damaged in several other cases [10], and stair damage was also observed in some steel frame structures as well [11]. Interior wall and ceiling systems [12] and exterior façade systems [13], which can protect against interior and exterior fire spread within buildings, were shown as being prone to significant damage, with façade damage in particular observed across numerous types and ages of buildings and façade systems [13]. Overall, the non-structural building systems, including ceiling, façade, and fire protection systems, are reported as contributing a significant percentage of the NZ\$16 Billion loss in the Christchurch earthquakes [13]: a fact that unfortunately has been demonstrated in several other earthquake events as well [14–17].

Data such as these clearly show that more work is needed to improve the seismic performance of nonstructural systems: not only those which can result in high direct and indirect monetary losses, but those which can impact safety to occupants and first responders, particularly fire safety systems. To better understand, characterize and predict the potential damage to building nonstructural components and systems during earthquakes and post-earthquake fires, a series of earthquake motion tests and post-earthquake fire tests was conducted on a full-scale, five-story building specimen, which was equipped with various nonstructural components and systems and contents reflective of medical, computer server, office, residential and utility spaces [18–30]. The experiments were performed on the large high performance outdoor shake table (LHPOST) at the Englekirk Structural Engineering Center of the University of California, San Diego [31]. Referred to as the BNCS Project (Building Nonstructural Components and Systems Project), this unique collaboration between academia, government, and industry was developed with the aim to expand on the knowledge of the performance of the NCS during earthquakes and post-earthquake fires. Various aspects of the research program, partners and outcomes can be found at the project website (<http://bncs.ucsd.edu/index.html>) and in the literature [18–30]. The following summarizes and synthesizes key outcomes of this research and illustrates how they can be used within a conceptual framework for integrating seismic and fire protection engineering (Figure 1).

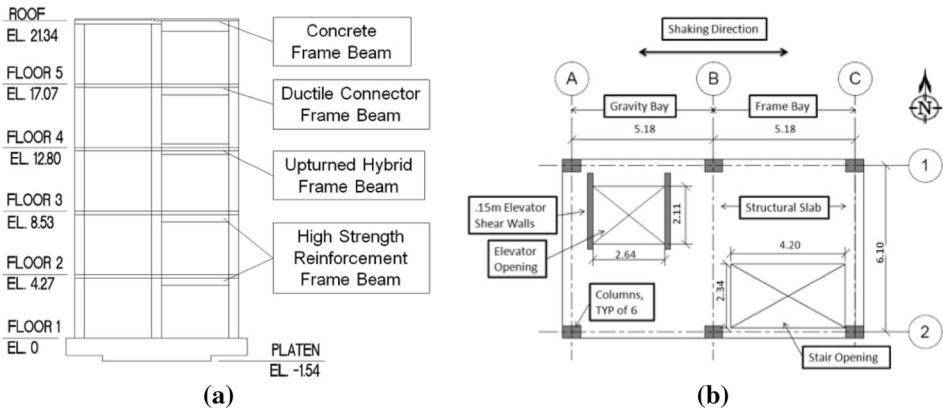


Figure 1. Test specimen: schematic of (a) elevation view and (b) plan view [24, reprinted with permission from ASCE].

2. Test Specimen

2.1. Structural System

The building test specimen, designed as a flexible frame-braced structure with characteristics common in mid- to high-rise buildings, was constructed of poured in place concrete at full-scale with five floor levels. Floor-to-floor heights were 4.27 m (14 feet) at each level, resulting in a total height of 21.35 m (70 feet). The specimen featured two bays in the longitudinal (shaking) direction and one bay in the transverse direction [19, 24]. With a floor plan of 6.6 m (21.6 feet) by 11.0 m (36 feet), the specimen occupied the complete shake table platen at the LHPOST facility. The structural system was designed based on a performance target of around 2.5% maximum lateral inter-story drift ratio with a maximum peak floor acceleration (PFA) of around 0.7 g to 0.8 g [18]. Additional details can be found in [18, 19, 24].

2.2. Nonstructural Components and Systems

The building test specimen was fully outfitted with a broad array of nonstructural components and systems, including a working elevator, full sized prefabricated metal stairs, various interior partition and ceiling systems, two configurations of exterior cladding, operational electrical, lighting, fire sprinkler, and fire detection systems, operational fire dampers, mechanical ventilation ductwork, a water filled cooling tower and a fixed air handling unit. Contents included material and equipment representative various building uses. In particular, levels four and five of the specimen reflected an intensive care unit (ICU) and surgery suite, respectively, level three reflected office space and featured two large computer servers anchored to the slab, level two was detailed with dual occupancies of laboratory and residential space, and the level one was a designated as a utility floor. Additional details can be found in [18, 19, 24].

2.2.1. Architectural and Egress Systems The building test specimen frame was enclosed using two architectural façade systems. The first three levels were enclosed by a balloon framing system comprised of lightweight steel studs, gypsum board interior faces and an exterior insulation and finishing system (EIFS), while the top two levels were enclosed with precast concrete panels. The interior of the balloon frame façade was lined with 16 mm (5/8 inch), fire-rated, Type X gypsum board, as were interior partition walls, providing an equivalent of a 1-h fire rating. Interior partition walls were also framed with lightweight steel studs [19]. Swinging doors with automatic door closers and magnetic door hold open devices were installed between compartments on Floor 3. The doors were 910 mm (3 feet) wide, 2100 mm (7 feet) high and 35 mm (1-3/8 in) thick, composed of a 13.6 kg (30 pound) particleboard core with hardboard cover [23]. The door hardware consisted of standard duty commercial cylindrical lever locks-grade 2. The door latch was made of 3-h fire rated stainless steel. A roll-down fire door, with fusible link activation temperature of 74°C (165°F) was installed between compartments SBR and LBR on Floor 3 [23, 28]. Ceiling systems were installed in the Northeast and Southeast portions of each floor, with different systems installed on each level. The ceiling system on Floor 3, which is where the fire experiments were conducted, consisted of a gypsum board grid system, using 16 mm (5/8 inch), fire-rated, Type X gypsum board [19, 23], providing a nominal 1-h fire rating. Figure 2 presents the architectural layout of Floor 3. The room designations reflect fire test areas: small burn room (SBR), large burn room (LBR), elevator shaft area (ES) and elevator lobby area (EL).

A prefabricated stair assembly was installed at each floor of the specimen. Each floor consisted of lower and upper flights and an intermediate landing. The stair flights were connected with the concrete floor slabs at one end via field welds, while they were connected with a stair landing via bolts at the other end. A fully

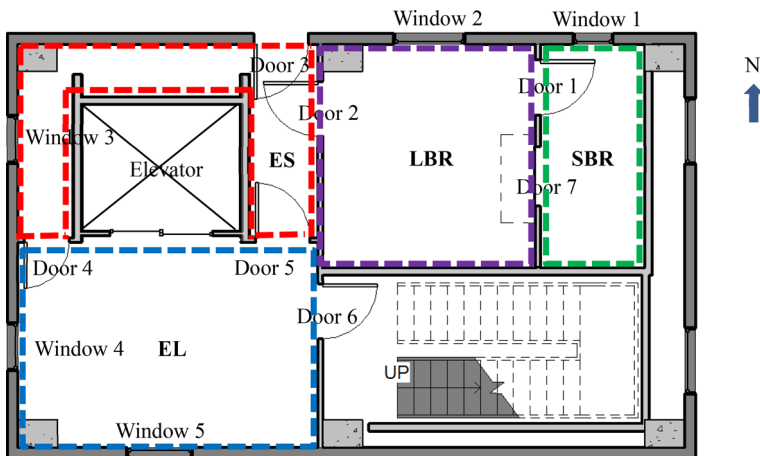


Figure 2. Layout of Floor 3 [23].



Figure 3. Photographs of (a) the façade systems on the BNCS test specimen, (b) stair enclosure looking onto Floor 3, and (c) partition wall and door on Floor 3 [19, 23].

functioning elevator with 17.1 m (56.1 feet) travel height and access to all floors was installed in a 2.64 m (8.6 feet) by 2.1 m (6.8 feet) elevator shaft. The elevator shaft was enclosed using two layers of 16 mm (5/8 in) Type X fire rated gypsum board, providing a nominal 2-h fire rating. The EL on each level was enclosed using one layer of 16 mm (5/8 in) Type X fire rated gypsum board, as was the stairwell on several levels, for a nominal 1-h fire rating. During the seismic tests, the 1.92 m (6.3 feet) by 1.7 m (5.6 feet) by 2.36 m (7.7 feet) cab was loaded with sand bags equivalent to 40% of the full cab capacity of 160 kg (352.7 pounds). The opening of the cab door was 2.1 m (6.8 feet) by 1.1 m (3.6 feet). Photographs of select architectural features are shown in Figure 3 [19, 23]. Additional details can be found in [18, 19, 23–25, 29].

2.2.2. Fire Protection Systems A functional wet pipe automatic fire sprinkler system was installed throughout the building test specimen. Risers [6.35 cm (2½ in)] and control valves were installed adjacent to the West wall of the elevator shaft at each floor level, with several variations of branch and loop configurations and pipe materials on each level [28]. All horizontal sprinkler branch and loop lines were installed 30 cm (12 in) below the deck of the floor above. Variations in pipe material and layout were installed to assess performance of the different configurations under seismic load. The design was compliant with applicable building code requirements. Details on the sprinkler system design, including calculations, components and layout, can be found in [23]. A photograph showing some installed sprinkler system components can be found in Figure 3a. To obtain realistic seismic performance, while minimizing any possible water damage to equipment for potential pipe rupture, the system was charged with only 284 l (75 gallons) of water and pressurized to 221 kPa (32 psi) during motion tests [28].

Sheet metal heating, ventilation air-conditioning (HVAC) ductwork, including operational 1.5-h rated (UL 555) fire and smoke dampers, was installed on Floor 3 and vented to the outside through a vertical duct on Floor 4 [23]. Flexible duct connections, which were in the above ceiling plenum space, were installed between

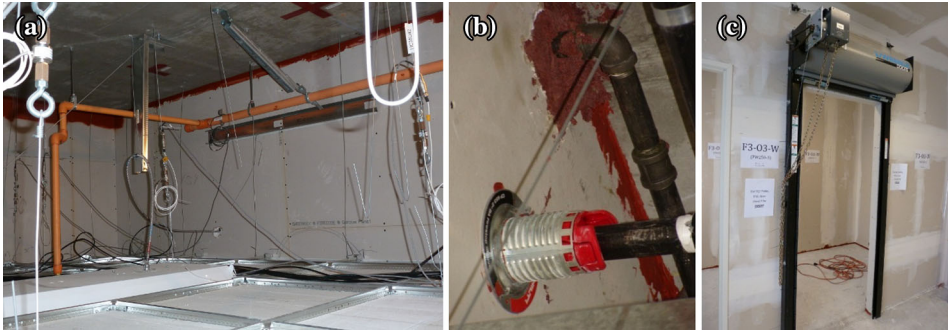


Figure 4. Photographs of (a) above ceiling space showing sprinkler piping and brace, fire seal and ceiling system on Floor 2, (b) representative firestop systems on Floor 3, and (c) fire door and partition walls between compartments on Floor 3 [23].

the sheet metal ducts and the room air diffusers located in the Floor 3 ceiling. The fire dampers were located in the ductwork penetrations of the Northeast compartment partition walls. Penetrations in compartment walls on Floor 3, including openings for sprinkler piping, HVAC ducts, electrical conduit, and a cable tray, were firestopped with a range of fire sealants, caulking and firestop systems. In total ten different fire sealants, caulking and firestop systems were installed throughout the specimen building [23]. A number of firestop systems can be seen in several of the photographs provided in Figures 3 and 4.

3. Instrumentation

The building test specimen was outfit with a diversity of analog sensors, digital video cameras and a global positioning system (GPS). For the seismic testing, a total of 515 analog sensors and 87 digital video cameras were deployed [19, 21, 24]. About one-third of the sensors and cameras were utilized to monitor the structural skeleton, with most associated with a dense accelerometer array composed of four tri-axial force-balance accelerometers per floor (one at each corner), with the remaining two-thirds, including about 100 displacement sensors, 60 load cells, 20 strain gages, and 140 accelerometers, installed on various nonstructural systems and components. Select systems, such as the egress, interior compartmentation and facades, were more densely monitored than others due to the size, lack of prior data, and complexity [24]. A network of 56 IP and 16 military-grade co-axial digital cameras were distributed within the building, with HD camcorders (hand-held cameras) and HD GoPro cameras (mountable or wearable, such as on helmets) used to collect visual data from various exterior locations. Additional details can be found in [21].

For the fire tests, thermocouples (TCs) were placed in various locations, including within the fire compartment, along compartment joints and firestop systems, and at various locations outside of the compartment. A total of 96 TCs were used in each fire test, being located as appropriate to compartment geometries, fire pro-

tection systems being monitored, such as firestop system and sprinkler heads, location of gaps opened up by the motion tests, and specific features of the space. In addition to monitoring conditions inside of the fire compartments, the aims were to assess the potential for fire and smoke spread between compartments as a result of seismic-induced compartment integrity failure and to assess the performance of the fire protection systems. In addition to the TCs, multiple video cameras were installed throughout the building, including inside and outside of the fire compartment, to collect visual data on smoke or fire spread, and activation of the fire protection systems. Additional details can be found in [21, 23].

4. Design Ground Motions/Test Parameters

Seismic motions were selected from earthquake events which occurred off the coast of California, in the central area of Alaska and the subduction zone of South America, as these motions provided excitations with different frequency content distributions as well as varied strong motion durations and amplitudes [19, 24]. These were applied to the test specimen under two configurations: base isolation (BI) and fixed-base (FB). The FB configuration represents the condition where the building is connected to the ground via the foundation. When an earthquake occurs, energy is transmitted to the building, generating potentially significant forces and displacement. BI systems essentially decouple the building from the ground, absorbing energy and reducing forces and displacement transmitted to the building. The BI test series (seven motions, BI-1 to BI-7) was conducted first. This was to keep damage to a minimum for the FB test series (six motions, FB-1 to FB-6). Details regarding the BI system can be found in [19].

To preserve the structure for the FB testing phase, it was desirable to minimize the peak inter-story drift ratio (PIDR) to less than approximately 0.5% during the BI phase, while during the FB phase the design event was intended to achieve approximately 2% to 2.5% PIDR and 0.8 g PFA in the specimen [19, 32]. The achieved peak input accelerations for the FB earthquake motions ranged from about 0.2 g to 0.8 g, while the pseudo-spectral acceleration at a period of 1 s, approximately the elastic fundamental mode of the building while fixed at its base ranged from about 0.3 g to 1.3 g [24]. PFA and PIDR for the BI and FB tests are summarized in Figure 4. Details of design motions and measured responses can be found in [19, 20] and are summarized in [24].

5. Damage Resulting from Ground Motions and Implications for Fire Safety Designers

The largest ground motions (FB-5 and FB-6) induced damage to nearly every structural and nonstructural system in the test specimen. Damage to the structural system included densely concentrated cracking in the slabs around columns resulting in punching shear failure, concrete spalling at the base of columns and the ends of beams where the large rotations occurred, as well as fractured and yielded longitudinal rebar in the Floor 2 and Floor 3 frame beams, which required several

floors to be shored up prior to fire testing [20, 24, 25, 28]. Representative damage is shown in Figure 6a. Such damage to the structural systems has obvious concerns for stability of a structure following an earthquake. However, the earthquake-damaged components are more also susceptible to failure in a post-earthquake fire situation. Systems with spalled concrete, exposed or fractured rebar will not have the intended fire resistance and performance during a fire, if such damage was not considered.

The façade systems experienced different levels of damage, with significant damage to the balloon framed exterior system and minor cracking of the precast concrete exterior system. During FB-5, where the peak IDR was 2.8%, the balloon framing was severely damaged. The damage to the two ends of the building moving out-of-plane (OOP) with respect to the direction of motion input was much less than that observed on in-plane sides and partly caused by the interaction with other damaged systems [25]. A major concern with damage to façade systems is the potential for vertical fire spread during post-earthquake fires, which could occur between gaps that open between the floor slab and façade, or if parts of the façade fail in such a way as to provide significant openings to the outside. Glazing systems were not tested as part of façade systems in the BNCS tests due to funding issues. However, breakage of windows and glass façade components has been oft observed in earthquake events (e.g., see [13]), so such an outcome could readily be expected for some systems and materials (Figure 5).

Damage to interior partition systems varied widely, with gypsum wallboard being shaken off the walls in some cases, and only cracking and minor openings in joints observed in other locations [20, 23, 25]. Doors in partition walls were in some cases jammed shut, while in others were not able to be closed. Assemblies moving OOP with respect to the direction of motion generally suffered greater damage. The various ceiling systems also exhibited a range of performance, with damage to supports and ceiling tiles on some floors and little damage to systems on others. Damage to interior partitions and ceilings is of particular relevance to fire safety performance, since such systems are integral to fire compartmentation and egress systems. If partition walls and ceiling systems are breached, gaps will allow air to enter compartments, which can enhance burning. Perhaps more importantly the gaps will allow for the spread of smoke and fire, defeating the intended means of protection (compartmentation) and resulting in untenable conditions to develop remote from the fire location. Representative damage is illustrated in Figure 6b.

In order to gain some insight on the relationship between ground motion intensity and compartment damage, room integrity tests were conducted in the SBR and combined LBR + SBR compartments on Floor 3 (see Figure 2). These spaces were selected as they were outfitted to meet fire and smoke compartments, including firestopping of all through penetrations and dampers in ductwork. Room integrity tests measure gross leakage area in compartment boundaries by measuring pressure differentials between the outside and inside of the compartment under investigation. They are sometimes utilized for smoke barrier and stair pressurization system testing and qualification. In this case, a blower door fan was used to provide an indication of the total leakage area resulting from cracks and gaps formed in walls, ceilings and at joints during the motion tests [23, 26, 28].

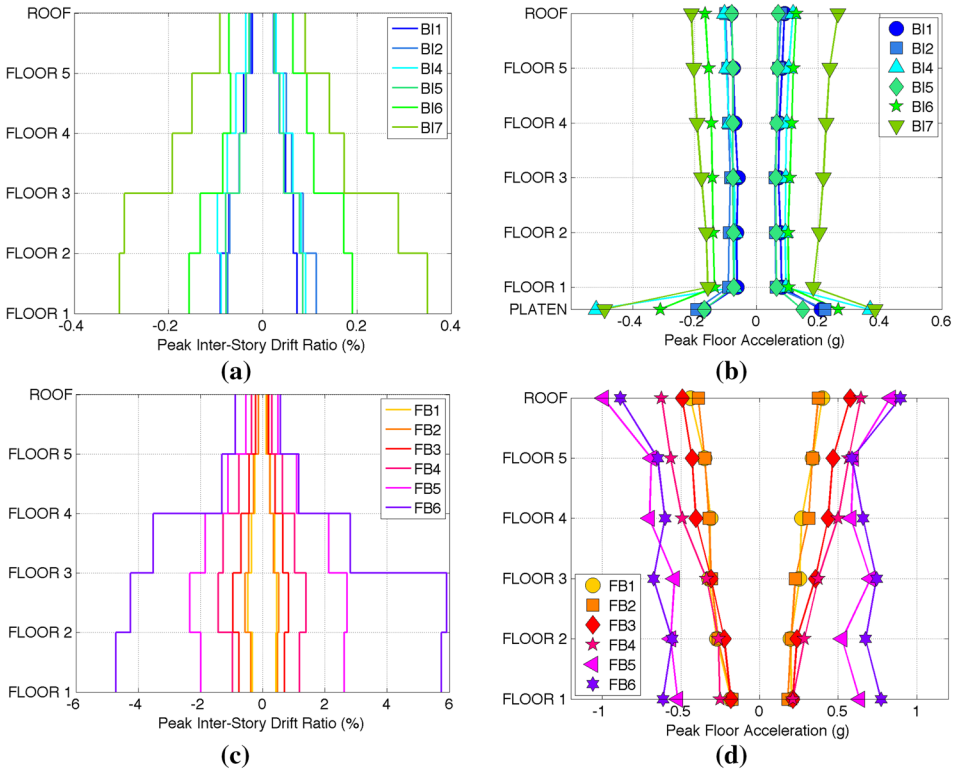


Figure 5. Peak floor acceleration (PFA) and peak inter-story drift ratio (PIDR) for (a), (b) the BI testing phase and (c), (d) the FB testing phase [24, reprinted with permission from ASCE].

Air velocity measurements allowed for gauging of air flow rates and for identifying the specific locations of leaks. Fan flow and compartment pressure readings were obtained using a manometer. These data were then used to determine the effective leakage area and the air change rate. The relationship of the flow and pressure can be expressed empirically as

$$Q_f = \kappa P_f^n \tag{1}$$

where f is a fan induced flow or pressure, Q is a airflow rate, P is a pressure, κ is a leakage coefficient.

Equation 1 can be simplified to show the effective leakage area of an orifice as:

$$Q_f = ELA \sqrt{\frac{2P_f}{\rho}} \tag{2}$$

where ELA is a effective leakage area, ρ is a density of air.

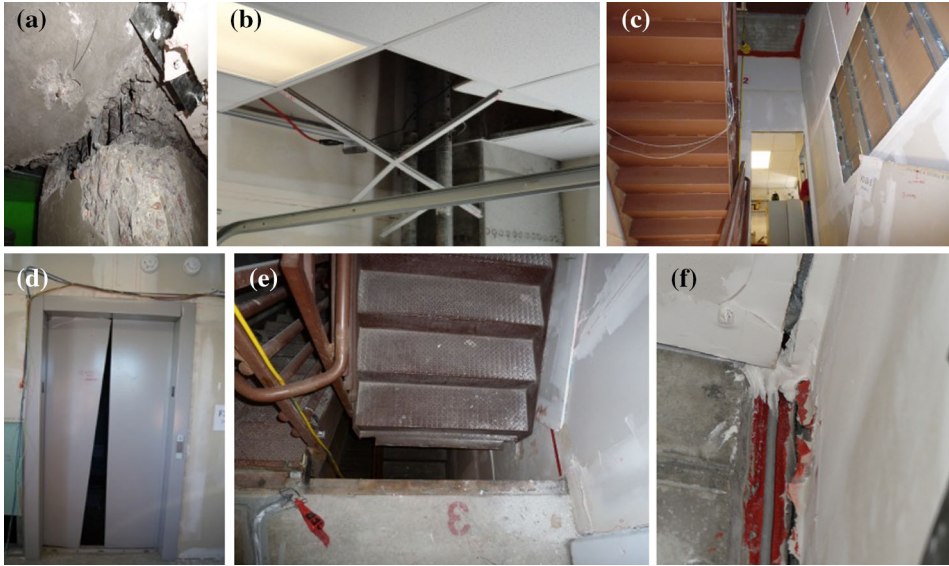


Figure 6. Examples of damage following FB-6 (a) beam-column connection failure on Floor 2, (b) ceiling damage on Floor 1, (c) loss of gypsum wallboard in stairwell approaching Floor 2, (d) distorted elevator door on Floor 3, (e) stair detached from landing at Floor 3, and (f) gaps in ceiling-wall and wall-column joints on Floor 3.

Testing indicated that for the smaller ground motions (all BI and FB-1 to FB-4), little increase in leakage area resulted. However, as a result of FB-5, the total leakage area in SBR increased by almost 300% as compared with pre-motion baseline, and by almost 900% following FB-6. The type of damage included gaps at joints of up to 12 mm (0.5 in), as illustrated in Figure 6f. While this particular test series was limited in scope due to time and resource constraints, it illustrates the extent of damage which can occur for construction of this type. Significantly larger increases in leakage area could be expected with other systems, such as the drop-in ceiling system installed on Floors 1 and 2 of the test specimen, which had significant failures (e.g., see Figure 6b). Details can be found in [23, 26, 28].

The elevator doors on Floors 2 and 3 were damaged during FB-6, resulting in a triangular-shaped opening on each level of about 0.3 m², rendering it unusable and creating an unprotected opening between floors via the elevator shaft [20, 23, 25, 28]. The stairs became disconnected from the landings at Floors 3 and 4, with handrail weld fractures in some locations. Damage to elevators and stairs have obvious implications for occupant egress and emergency responder access. If a building fire performance analysis does not consider the potential for these systems as unavailable during a post-earthquake fire, egress times and emergency response times can be significantly underestimated, which could have a significant

impact on the prediction of occupant and emergency responder safety. Damage to the elevator door and stairs is shown in Figure 6d, e.

The sprinkler system and the various firestop systems generally performed well. There was clear displacement of the sprinkler riser in some locations, but no leaks or loss of pressure [20, 23, 25, 28]. While the sprinkler system performed well, it is worth noting that the hangars, bracing and other components were installed in accordance with current regulatory requirements, which may reflect a higher degree of performance than older, existing systems. Recent testing of sprinkler and ceiling systems at the University of Buffalo points to sprinkler performance considerations for earthquake prone buildings [33, 34]. Most firestop systems were undamaged; however, those systems designed for static joints, which were subjected to the dynamic movement of the specimen, were damaged as gaps opened at connection points (e.g., wall to wall, wall to ceiling) [20, 23, 25, 28]. This can be seen in Figure 6f. This situation does not appear to be addressed in current building regulations and design practice.

During FB-5 and FB-6, contents of various types and sizes, which were not anchored, were displaced, and in some cases anchored contents were displaced [20, 28]. There are two major concerns with displacement of contents: changing the configuration and potential burning characteristics of fuel, and blocking means of access or egress. Selection of design fire for fire performance analysis includes assumptions about location, type and configuration of fuels. If one assumes, for example, an office space with books packed tightly in an upright bookcase, that will reflect a much different fire than a situation with the books scattered on the floor with the bookcase (potentially combustible) on top. With respect to egress and access, large items can block paths of travel, including access to elevators, stairs and doorways. This impacts both occupant egress as well as emergency responder access, and should be considered in building fire performance analyses.

Comparing the BNCS tests and outcomes to reported data on earthquake intensity levels and resulting damage (e.g., [5, 7, 9–17, 35, 36]), the BNCS test specimen was subjected to motions within the range of reported earthquakes and testing, and damage outcomes were similar. The automatic sprinkler system generally experienced less damage than reported in Japanese earthquakes, which could be due to different sprinkler standards, including increased seismic restraint requirements. Damage to doors was similar. While damage to compartmentation and stairs was unable to be compared to Japanese and US data, testing of earthquake damaged fire compartments in New Zealand [37] and outcomes from the 2010 to 2011 Christchurch earthquakes [10–13] suggest damage levels are similar, and at the very least, a concern.

6. Design Fires/Test Parameters

A series of six room-scale fire tests were conducted following the last motion test in order to evaluate the fire performance of the earthquake-damaged specimen. The focus was evaluation of passive and active fire protection systems and features, including compartment integrity, firestop performance, damper perfor-

mance, smoke detector performance and sprinkler performance. Key guiding criteria were to achieve sufficiently high temperatures to activate firestop systems, and sufficiently large fires to assess smoke and fire spread potential. It was not possible to assess structural fire performance due to limits imposed on the testing, including environmental restrictions on burning of actual building contents, limitations on size of the fire and extent of potential damage to the building, both for life safety and shake table damage concerns, limited funding, and limited time available to conduct the tests prior to demolition of the specimen and before the wildland fire season began. With respect to the sprinkler system, the intent was simply to evaluate activation of the sprinkler, and not the suppression or control aspects, as the fires were needed to assess other attributes.

In order to achieve the experimental objectives and to comply with the various constraints identified above, it was determined that minimum gas temperatures needed to reach at least 250°C (482°F), maximum burn times were limited to 15 min, flashover or near flashover conditions were desirable, and visible smoke was desirable. Given the various compartment and ventilation characteristics, it was determined that the resulting fire sizes needed to range of approximately 500 kW to 2000 kW. Heptane was selected as the fuel, and it was decided to use multiple small steel pans to achieve various fire sizes needed for the test compartments [23, 27]. Pans were sized at 0.6 m (2 feet) by 0.4 m (1.3 feet), which based on the following steady-state mass burning rate correlation and associated constants [38], would result in about a 500 kW fire in each.

$$\dot{q} = \Delta h_c \dot{m}''_{\infty} (1 - e^{-k\beta D}) A$$

where Δh_c is a heat of combustion ($=44.6$ MJ/kg), \dot{m}''_{∞} is a mass burning rate ($=0.101$ kg/m²-s), $k\beta$ is a corrected extinction coefficient ($=1.1$ m⁻¹), D is a effective pan diameter ($=0.55$ m, $A = \frac{\pi}{4} D^2$), A is a surface area ($=0.24$ m²).

To control against potential spillage, each heptane fuel pan was located in a steel retention pan. For each test, the fire size and duration was established based on the number of fuel pans in the compartment and the amount of heptane placed in each pan. To help assure benchmark required fuel and resulting heat release rates, a preliminary test was conducted in the WPI fire laboratory, using 9 l of heptane. As measured under the large oxygen depletion calorimeter, the resulting HRR curve is shown in Figure 7. The average HRR of about 510 kW throughout the effective burning time of 9.5 min was in a good agreement with the design calculations.

The locations of the fire tests, and number of heptane pans, are shown in Figure 8 [23, 27]. For all tests the sprinkler system was charged at a pressure of 221 kPa (32 psi) and the system in the third floor was disconnected from the rest of the floors. The primary purpose and test conditions of each of the fire tests are detailed in [23] and summarized in [27].

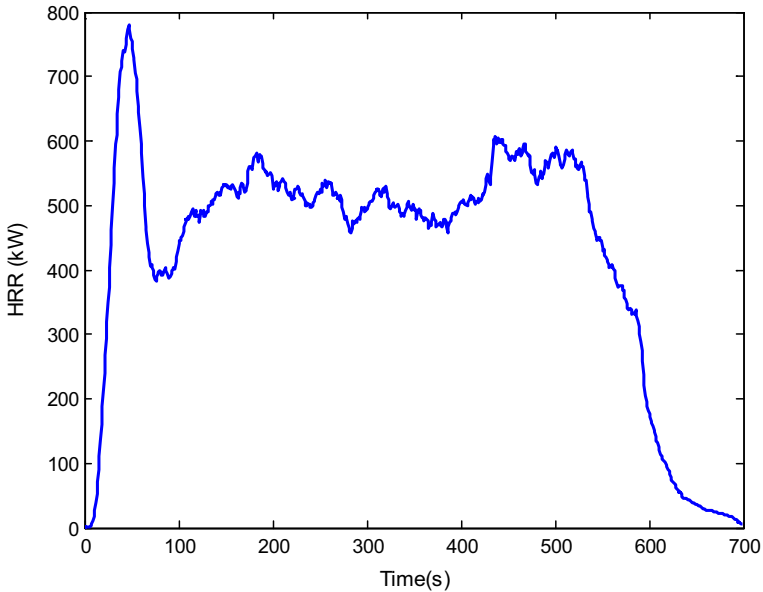


Figure 7. HRR curve of 9L heptane pan fire as measured in WPI laboratory [23, 27].

7. Outcomes from Fire Tests

In general, the fire protection systems, which were undamaged by the motion tests, performed well during the fire tests. This includes the fire sprinklers, fire dampers, roll-down fire door, smoke detectors, and several types and locations of firestop systems. Details can be found in [20, 23, 27]. Particular attention is given below to fire performance associated with gaps in partition walls and wall/ceiling connections, the damage to the elevator doors, the performance of firestop systems, and the performance of HVAC components.

With respect to compartmentation, the primary focus were the SBR and LBR, which were outfit as fire resistive compartments, with fire-rated wall and ceiling assemblies. Following the FB-6 motion test, a gap of about 25 mm had opened along the joint where the separating wall between the SBR and the LBR connected to the exterior wall on the North side. During the LBR-2 fire test (no ventilation openings other than motion-induced gaps: about a 1000 kW fire), smoke and flame was observed extending through this gap from the LBR into to SBR. Fire spread into SBR did not occur due to brevity of the test and the lack of fuel items being present in the SBR. However, given the observed flame extension and measured gas temperatures near the gap in excess of 350°C (662°F) for more than 1 min (Figure 9a), easily ignitable fuels in the vicinity could have been ignited if present [23].

While the elevator performed well up until FB-6, this final motion test caused the elevator door on Floors 2 and 3 to become significantly damaged, resulting in

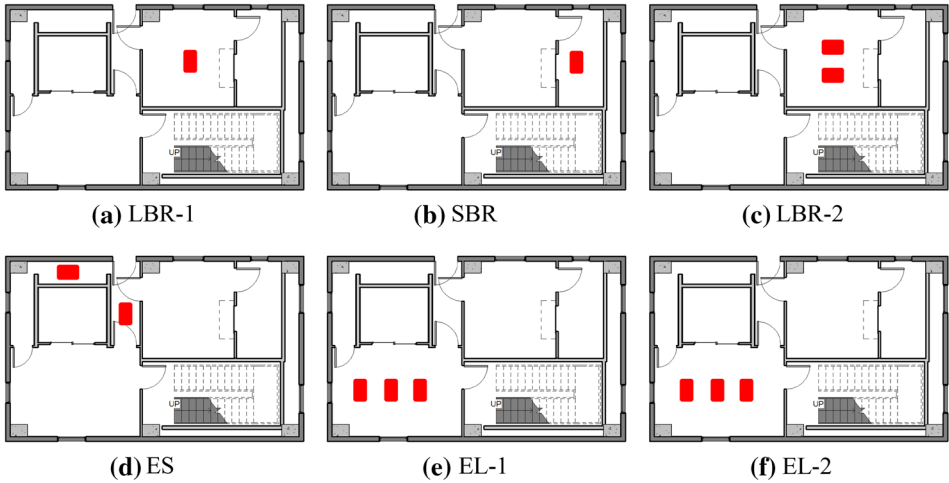


Figure 8. Fuel locations in each area with red box representing a heptane pan [27] (Color figure online).

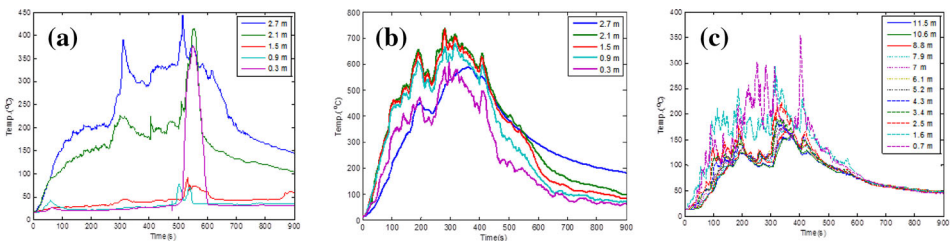


Figure 9. Flame extension from LBR to SBR (a) and temperature profile along gap between LBR and SBR (b) during LBR-2 fire test [23].

a triangular-shaped opening on each level of about 0.3 m^2 (see Figure 6d). To assess the potential for fire and smoke spread through the elevator shaft, given this opening into the shaft due to the damaged doors, tests EL-1 and EL-2 were conducted using three heptane pans placed in front of the elevator doors on Floor 3. For test EL-1, window openings in the EL were partially covered (window opening area of about 0.7 m^2) and the swinging doors to the lobby were fully closed. A thermocouple tree with 5 TCs was located in the EL, and a thermocouple string with 12 TCs was deployed in the elevator shaft, to collect associated temperature data. Resulting gas temperatures at various heights in the EL and in the elevator shaft are shown in Figure 9b, c. In the elevator shaft, the highest temperature, about 350°C (662°F), was recorded near the fire source, 0.7 m (2.3 feet) above the floor (Floor 3). Relatively uniform temperatures were observed throughout the shaft at heights corresponding to levels 4 and 5 [from 5.2 m (17 feet) to 11.5 m (37.7 feet)], with peak gas temperatures in this region ranging

between 150°C (302°F) and 200°C (392°F). While such temperatures may not be high enough to cause ignition of materials in the shaft (e.g., cables), it should be remembered that the fire size was small and the duration short, so much higher temperatures would be expected for larger and longer burning fires. This suggests that for higher energy, longer duration fires, piloted ignition of materials in elevator lobbies and flame spread could be possible via the shaft to upper floors. In addition, a significant amount of smoke spread was observed to the Floors 4 and 5 via the elevator shaft during this test as well, as evidenced by soot deposits on the concrete shaft wall and elevator door edges on those floors (see [23, 27] for more detail).

In general, firestop systems worked well. Examples are shown in Figure 10. The only observed problems were associated with fire sealants and similar systems, design for static joints (e.g., wall joints), which moved during the earthquake motion tests (e.g., see Figure 6f).

Various components of the mock heating, ventilation and air-condition (HVAC) system were assessed during. In the LBR-2 fire test, in which the upper gas temperature reached over 800°C (1472°F), the flexible duct connecting the ceiling diffuser in LBR to the metal duct and damper at the corridor partition wall was ruptured during the test. The temperature profile and damaged duct are shown in Figure 11. The legend in Figure 11a indicates the heights above the floor surface, with solid and dotted lines for the spaces above and below the ceiling, respectively. Despite the good performance of the fire-rated ceiling assembly during the ground motion tests and the LBR-2 fire test, the failure of the flexible duct during the fire test allowed hot gases into the plenum space.

Since no previously-reported data were found for fire and smoke spread in earthquake damaged buildings from full-scale testing, this aspect of the BNCS outcomes could not be directly compared with past experience. However, the BNCS tests illustrate that significant potential exists for smoke and fire spread due to the potential for compromised compartmentation and fire protection systems, which is consistent with past events and experiments (e.g., [5, 7, 9–17, 35, 36]).

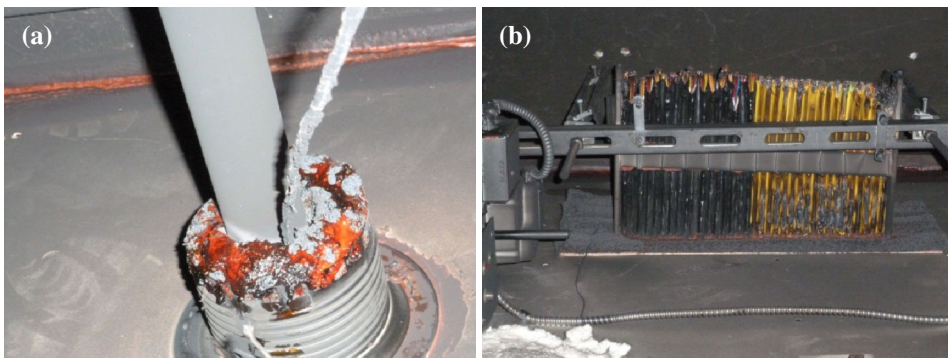


Figure 10. Horizontal pipe firestop in corridor (a) and Cable tray firestop in corridor (b) following ES fire test [23].

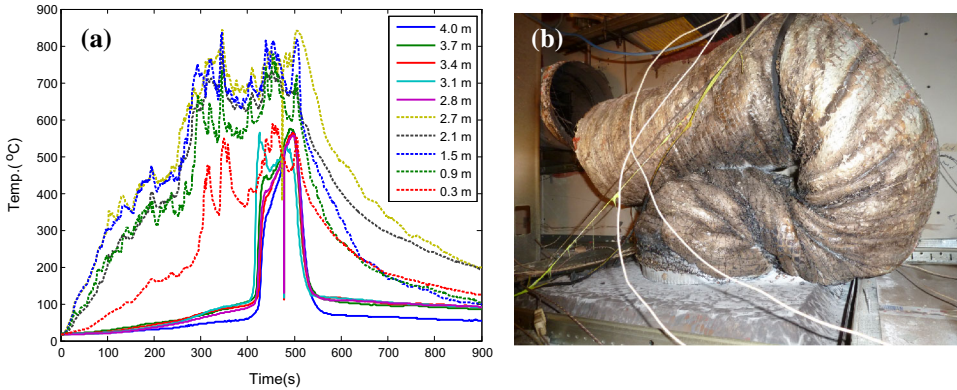


Figure 11. Temperature increase in the space above LBR ceiling (a) and flexible duct rupture (b) [27].

8. Conceptual Framework for Integrating Risk-Informed and Performance-Based Seismic and Fire Engineering

Using knowledge gained from the BNCS tests described above, and supplemented through investigation into performance-based approaches to earthquake engineering and fire engineering, a conceptual framework for an integrated, performance-based approach to earthquake and fire engineering has been outlined [30, 39]. It suggests merging the performance-based seismic design approach embodied in the work of Applied Technology Council (ATC), Project 58 [40], with the performance-based fire protection design approach outlined by the Society of Fire Protection Engineers (SFPE) [41], allowing one to obtain estimates on structural and nonstructural damage resulting from an earthquake as input for fire scenarios and fire protection systems reliability estimates for post-earthquake building fire performance analysis.

In brief, the ATC-58 guidelines [40] outline a performance-based approach for seismic design (PBSD) of new buildings or design of seismic upgrades for existing buildings with the specific intent that the buildings be able to achieve specified performance as related to the amount of damage the building may experience and the consequences of this damage including, potential casualties, loss of use or occupancy, and repair and reconstruction cost. Performance objectives reflect statements of the acceptable risk related to incurring damage or loss for identified earthquake hazards [40]. Given the performance objectives, seismic engineers develop the design to a sufficient level of detail to allow determination of the building's performance characteristics, which for new buildings will include as a minimum identification of: (1) the location and characteristics of the site; (2) building size, configuration and occupancy; (3) type, location and character of finishes and nonstructural systems; (4) selection of structural system type and configuration; and, (5) developing estimates of the strength, stiffness and ductility of this system. Seismic engineers then conduct a series of structural analyses to predict the building's response when subjected to the earthquake hazards and use the

information obtained from these analyses to assess the amount of damage that may occur and the probable consequences of this damage, which is then compared to the desired performance. If the assessed performance meets or exceeds the target performance objectives, the design is deemed adequate. If not, either the performance objectives or the design need to be modified.

The performance-based fire safety design (PBFSD) process outlined by SFPE [41] requires clearly specified stakeholder goals and objectives (in terms of function, performance, and/or loss), design objectives (expectation of building performance under load), design fire scenarios and loads (from normal use or hazard events expected to impact the building), and performance/design/failure criteria (metrics to judge successful performance). It requires the building, occupants and hazards to be characterized, trial designs (mitigation measures) to be postulated and evaluated against the scenarios and loads in order to meet performance objectives. While conceptually similar to the PBS approach, the PBFSD approach is predominantly deterministic in nature, with probabilistic methods used primarily for scenario development, whereas the PBS approach is a probability based approach, considering scenarios, loads and responses probabilistically.

It is suggested that the PBS and PBFSD approaches can be integrated, since the same fundamental components exist in each. The primary issues which need to be addressed include at what point are data from seismic analysis and fire analysis incorporated, respectively, how best should acceptance criteria and representations of performance be stated, and from where are required data obtained. The conceptual framework for how seismic analysis and fire analysis might be incorporated is diagrammed in Figure 12. The main objective of the diagram is to illustrate where the direct and indirect relationships between earthquakes and fires existing as a function of the building. For given characteristics of a building, the diagram helps identify possible consequences from either a fire or an earthquake event and how the two events might interact.

The major attributes of hazards that can affect the building performance for each type of event are identified with red text in black colored boxes (earthquake or fire intensity and duration). Key building attributes that can influence performance are identified with black text in black boxes (e.g., construction material, quality of construction, fuel load, etc.). Outcomes of events (consequences) and are identified with red text in red boxes (e.g., damage to structure, damage to nonstructural systems, smoke development and spread, high temperatures, etc.). The building factors that may have a direct impact on certain consequences are related by dotted grey lines to show the connections. The red dotted lines are termed as 'secondary connections' and are mapped to show which consequences of post-earthquake building fire that a fire protection engineer should consider when developing fire safety designs for earthquake prone buildings. The components and connections are more fully described in [39].

For example, for any building under analysis in an earthquake-prone area, there would typically be separate earthquake performance and fire performance analyses undertaken. The earthquake analysis would characterize the hazard in terms of intensity and duration, and measure impacts associated with predicted drift and acceleration. Based on the structural design, building materials, and so

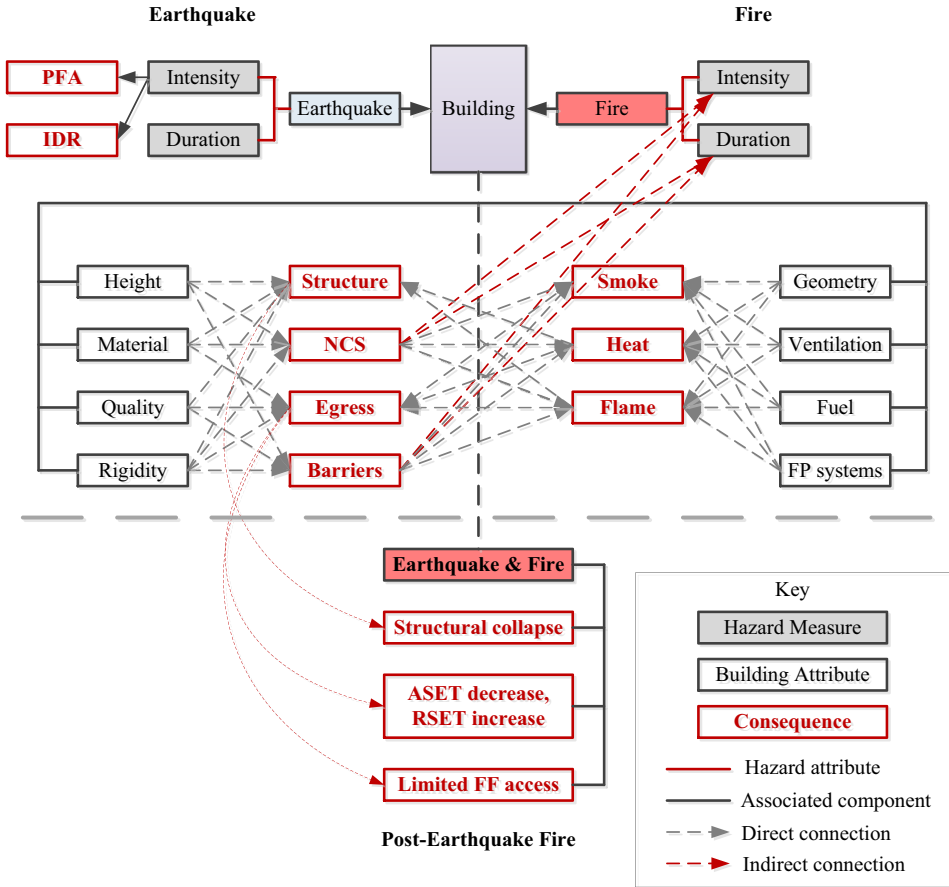


Figure 12. Conceptual model of integrated approach to performance-based seismic and fire design [30, 39].

forth, various damage estimates for the structure and building systems can be predicted. The fire engineering analysis would characterize the hazard in terms of fire intensity (HRR) and duration, and measure impacts in terms of predicted temperatures, tenability criteria, available and required safe egress times (RSET), structural failure criteria and the like. Based on compartment configuration, ventilation, fuel load, occupant load and the like, smoke and fire spread and impacts on people, property and mission can be predicted. The added step is to take the earthquake damage estimations from the earthquake engineering analysis and use that information to adjust building, occupant and fuel characteristics for the fire engineering analysis, factoring in such items as changes to fuel load distribution, ventilation (damaged windows/façade systems), compartmentation, fire protection, smoke control and lighting systems, availability of egress routes and similar impacts associated with the earthquake damage. This would then be used

to inform fire protection designs which are robust in the face of considered earthquake impacts.

While at present the fragility curves (probabilistic damage estimates) referenced in the ATC-58 approach are not all suitable for use in fire engineering analysis, they provide at least qualitative information about potential damage states. For example, the ATC-58 approach and associated Performance Assessment Calculation Tool (PACT) have fragility curves for damage to structural components and systems, façade systems, glazing systems, HVAC systems, partition systems and more, with respect to repair or replacement [40]. In addition, fragility curves on sprinkler systems [33, 34], ceiling systems [42], partitions [43] and other components continue to be generated. In concept, the PBSF approach can be applied to a building, fragility curves for various building components and systems will be generated, and these curves can be used as input to the PBFSD approach as reflective of the building (and systems) characteristics for which scenario analysis will then follow. This approach provides such information as: damage indication of façade, glazing and interior partition systems, which will impact the potential for spread of smoke and flame; damage to access and egress components and systems, which will impact occupant evacuation and emergency responder access; damage to fire protection systems (sprinklers, smoke control, etc.), which will impact tenability conditions; damage indication of structural systems, which will impact structural fire performance; and more.

The concept was applied to a fictitious shopping mall building in which available safe egress times (ASET) were compared to RSET in the PBFSD process, with and without consideration of earthquake induced damage [39]. It should be noted that at the time of this analysis, some of the fragility data, such as for sprinkler systems which have only recently been published, were not available [33, 34] and were not in the ATC-58 Performance Assessment Calculation Tool (PACT). Furthermore, since damage assessment within PACT is for replacement cost estimates, more so than fire performance, expert judgment was used to estimate damage as related to fire performance, such as the percent area of ventilation openings developed due to damage to ceilings, walls and glazing systems as a result of the design earthquake hazard. Likewise, distribution of fuel load was not anticipated in the PACT, so assumptions on this were made as well. PACT assumptions on loss of egress components, such as stairs, was used, and a combination of PACT assessments and assumptions was used to estimate injuries to people, which could impact ability to escape and time of movement.

Given the assumptions and limitations as outlined above, computational analysis of fire and smoke development and spread and of time to evacuate the building—in the undamaged and earthquake-damaged conditions—was simulated. For the fire effects analysis, PyroSim and FDS was used [44, 45], and for evacuation analysis, Pathfinder was used [46]. ASET and RSET estimates were developed for the undamaged and the earthquake-damaged mall building. A comparison of one set of ASET and RSET values is presented in Figure 13. The significant differences in the ASET are related to damage to compartmentation, differently distributed fuel loads, and damage to fire protection systems. Significant differences in RSET are related to loss of egress paths (stairs, in particular), decreased move-

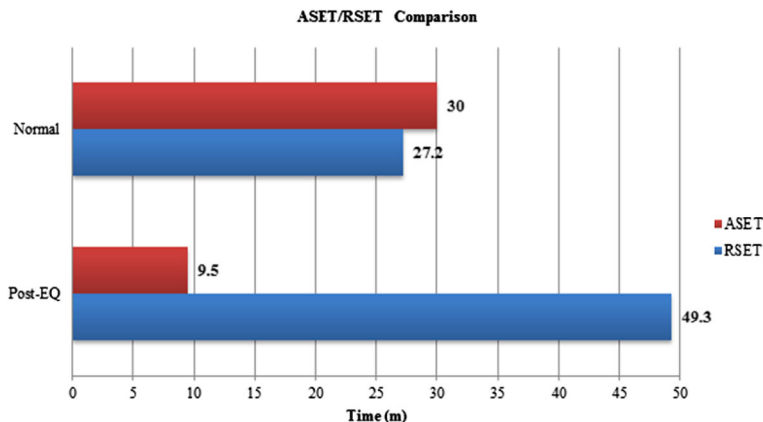


Figure 13. Comparison of building fire/life safety performance with and without earthquake damage consideration [39].

ment speeds due to debris [47], and related factors. While the outcomes should not be taken as absolute, especially given the limits on data availability and number of assumptions made, the magnitude of the difference in outcomes is significant, illustrating that at the very least earthquake damage should be considered when developing performance-based fire solutions to buildings in earthquake-prone areas.

9. Summary and Conclusions

The BNCS project was undertaken to better understand building nonstructural component and system performance during earthquakes and post-earthquake fires. The project illustrated that earthquake motions can compromise numerous fire safety systems and features. Compartment barrier components were compromised through gypsum wallboard becoming dislodged from walls, gaps opening at wall-to-wall and wall-to-ceiling joint areas, and damage to door frames and doors. Means of egress and access became blocked, damaged and in the case of the stairs and elevator, rendered unusable from the largest motions. Displaced contents and damaged ceiling components became impairments to travel. Damage to the structural system included densely concentrated cracking in the slabs around columns resulting in punching shear failure, concrete spalling at the base of columns and the ends of beams where the large rotations occurred, as well as fractured and yielded longitudinal rebar in the Floor 2 and Floor 3 frame beams, which required several floors to be shored up prior to fire testing.

The project outcomes also illustrated potential implications of post-earthquake fire. The damage to compartmentation and egress systems resulting from the ground motions allowed for the spread of fire, smoke and toxic products of combustion, and would have prevented building occupants from escaping. The combi-

nation of untenable conditions and no means of escape is a particularly significant concern. While most of the fire protection systems that were not mechanically damaged as a result of the motion tests, such as the automatic sprinkler system and roll-down fire door, functioned well, data from real events shows that these systems are susceptible to motion-induced damage as well. While most firestop sealants and systems activated as intended and prevented fire and smoke spread, the detachment of some firestop materials from static joints, which become dynamic due to significant inter-story movement, was identified. Since the differentiation between static and dynamic joints, with respect to firestop performance, may not be valid in earthquake conditions, it may be necessary to consider all joints for which fire and smoke spread control is required to be considered dynamic for buildings constructed in seismic zones.

The findings and observations from this project are not wholly unexpected, since they mimic damage from real events. However, what is concerning is that damage similar to what was observed from events 20 years ago and beyond was observed in a test specimen built to current codes and design methods in the U.S., and that integration of earthquake and fire engineering is still not being effectively addressed. To address the latter concern, a conceptual approach to integrating performance-based seismic design and PBFSD has been outlined and tested using a hypothetical building, earthquake and fire conditions. While it shows promise, considerably more research and development is needed to obtain fragility curves which function equally as well for both seismic and fire performance analysis, and to properly integrate the approaches into a single method. With recent advances in methods to predict the performance of buildings to earthquake and to fire, and ongoing research to develop fragility curves, there is some hope that an integrated approach might be available in the near future.

Acknowledgments

The BNCS project was a collaboration of four academic institutions, University of California, San Diego, San Diego State University, Howard University and Worcester Polytechnic Institute, with support from the National Science Foundation (NSF), the Englekirk Advisory Board, the Charles Pankow Foundation, the California Seismic Safety Commission, more than 30 industry partners and two oversight committees. Their participation and support is greatly appreciated. A full listing of industry project sponsors can be found on the project website: <http://bncs.ucsd.edu/index.html>. NSF funding was provided through the National Earthquake Engineering Simulation Research program under Dr. Joy Pauschke, program manager, through award CMMI-0936505. Support from this program is gratefully acknowledged. In addition, the technical support of NEES@UCSD staff, and consulting contributions from Robert Bachman, are greatly appreciated. Funding for the fire tests were provided by ARUP, Hilti, CSSC, The SFPE Educational & Scientific Foundation, and WPI. The authors very much appreciate the above technical and financial support. Special thanks are given to Dr. Haejun Park, Mr. Jin-Kyung Kim and Mr. A.J. Campanella for their efforts on this pro-

ject as students at WPI, to Professor Tara Hutchinson from UCSD as overall project leader for her tireless efforts in making the project a reality and a success, to the other lead investigators, Professors Jose Restrepo, Joel Conte and Ken Walsh, and to lead industry liaisons Matthew Hoehler and Robert Bachman. Special thanks are also given to ASCE for allowing reuse of material from ASCE publications [24–26]. Helpful comments from the anonymous reviewers is greatly appreciated. Any summaries, opinions, findings, conclusions or recommendations expressed in this report are those of the authors and do not necessarily reflect project sponsors, institutions, agencies or organizations.

References

1. Chung RM (1996). January 17, 1995 Hyogoken-Nanbu (Kobe) earthquake: performance of structures, lifelines, and fire protection systems, NIST Special Report SP 901, NIST, Gaithersburg. http://www.nist.gov/manuscript-publication-search.cfm?pub_id=908748
2. Ohnishi K (1997) Causes of the seismic fires following the great Hanshin-Awaji earthquake survey. In: Beall KA (ed) NISTIR 6030, U.S./Japan government cooperative program on natural resources (UJNR), fire research and safety, 13th joint panel meeting, vol 2, March 13–20, 1996, Gaithersburg, pp 337–344
3. Fire and Disaster Management Agency (2006) Report of the 1995 Hyogo-ken Nanbu earthquake
4. NIST (1994) 1994 Northridge earthquake: performance of structures, lifelines and fire protection systems, NISTIR 5396, NIST, Gaithersburg
5. Fleming R (1998) Analysis of fire sprinkler system performance in the Northridge earthquake, NIST-GCR-98-736, NIST, Gaithersburg
6. Scawthorn C (1996) Fire following the Northridge and Kobe earthquakes. In: Beall KA (ed) U.S./Japan government cooperative program on natural resources (UJNR). Fire research and safety. 13th joint panel meeting. 1997, National Institute of Standards and Technology, vol 2, Gaithersburg, pp 325–335. <http://fire.nist.gov/bfrlpubs/fire97/PDF/f97147.pdf>
7. LeGrone P (2004) An analysis of fire sprinkler system failures during the Northridge earthquake and comparison with the seismic design standard for these systems. In: Proceedings, 13th world conference on earthquake engineering, Vancouver. http://www.iitk.ac.in/nicee/wcee/article/13_2136.pdf
8. Chen S, Lee GC, Masanobu S (2004) Hazard mitigation for earthquake and subsequent fire. http://mceer.buffalo.edu/research/International_Research/ANCER/Activities/2004/chen_sw_mceer.pdf. Accessed 20 August 2007
9. Sekizawa A, Ebihara M, Notake H (2003) Development of seismic-induced fire risk assessment method for a building. In: Fire safety science—Proceedings of the seventh international symposium, international association for fire safety science, pp 309–320
10. Elwood KJ, Pampanin S, Kam WY (2012) 22 February 2011 Christchurch earthquake and implications for the design of concrete structures In: Proceedings of the international symposium on engineering lessons learned from the 2011 Great East Japan earthquake, Tokyo. <http://www.jaee.gr.jp/event/seminar2012/eqsympto/pdf/papers/178.pdf>
11. Clifton C, Bruneau M, MacRae G, Leon R, Fussell A (2011) Steel structures damage from the Christchurch earthquake series of 2010 and 2011, Bulletin of the New Zealand

- society for earthquake engineering, special issue 44, number 4. [http://www.nzsee.org.nz/db/SpecialIssue/44\(4\)0297.pdf](http://www.nzsee.org.nz/db/SpecialIssue/44(4)0297.pdf)
12. Dhakal RP, MacRae GA, Hogg K (2011) Performance of ceilings in the February 2011 Christchurch earthquake, Bulletin of the New Zealand society for earthquake engineering, special issue 44, number 4. [http://www.nzsee.org.nz/db/SpecialIssue/44\(4\)0377.pdf](http://www.nzsee.org.nz/db/SpecialIssue/44(4)0377.pdf)
 13. Baird A, Palmero A, Pampanin S (2011) Façade damage assessment of multi-storey buildings in the 2011 Christchurch earthquake, Bulletin of the New Zealand Society for earthquake engineering, special issue 44, number 4. [http://www.nzsee.org.nz/db/SpecialIssue/44\(4\)0368.pdf](http://www.nzsee.org.nz/db/SpecialIssue/44(4)0368.pdf)
 14. Villaverde R (1997) Method to improve seismic provisions for nonstructural components in buildings. *J Struct Eng* 123:432–439
 15. Taghavi S, Miranda E (2003) Response assessment of non-structural building elements. Report No. 2003/05. Pacific earthquake engineering research center, Richmond
 16. Kircher CA (2003) It makes dollars and sense to improve nonstructural system performance. In: Proceedings of ATC 29-2 seminar on seismic design, performance, and retrofit of nonstructural components in critical facilities, Newport Beach. Accessed 23–24 Oct 2003
 17. Phan L, Taylor A (1996) State of the art report on seismic design requirements for non-structural building components, NISTIR 5857, National Institute of Standards and Technology, Gaithersburg
 18. Chen M, Pantoli E, Wang X, Espino E, Mintz S, Conte J, Hutchinson T, Marin C, Meacham B, Restrepo J, Walsh K, Englekirk R, Faghihi M, Hoehler M (2012) Design and construction of a full-scale 5-story base isolated building outfitted with nonstructural components for earthquake testing at the UCSD-NEES facility. In: Proceedings, 2012 ASCE structures congress, ASCE
 19. Chen M, Pantoli E, Astroza R, Ebrahimian H, Mintz S, Wang X, Hutchinson T, Conte J, Restrepo J, Meacham B, Kim J-K, Park H (2013) BNCS Report #1: full-scale structural and nonstructural building system performance during earthquakes and post-earthquake fire—specimen design, construction, and test protocol, University of California, San Diego
 20. Pantoli E, Chen M, Wang X, Astroza R, Ebrahimian H, Mintz S, Hutchinson T, Conte J, Restrepo J, Meacham B, Kim J-K, Park H (2013) BNCS Report #2: full-scale structural and nonstructural building system performance during earthquakes and post-earthquake fire—test results, University of California, San Diego
 21. Pantoli E, Chen M, Hutchinson T, Restrepo J (2013) BNCS Report #3: full-scale structural and nonstructural building system performance during earthquakes and post-earthquake fire—camera and analog sensor details, University of California, San Diego
 22. Chen M, Pantoli E, Wang X, Mintz S, Hutchinson T, Hutchinson T, Restrepo J (2013) BNCS Report #4: full-scale structural and nonstructural building system performance during earthquakes and post-earthquake fire—construction details and technical specifications of specific subsystems, University of California, San Diego
 23. Kim JK, Meacham BJ, Park H (2013) Full-scale structural and nonstructural building systems performance during earthquakes and post-earthquake fire: fire test program and preliminary outcomes. Worcester Polytechnic Institute, Worcester
 24. Hutchinson T, Restrepo J, Conte J, Meacham BJ (2013) Overview of the building non-structural components and systems (BNCS) project. In: Proceedings, 2013 ASCE structures congress, ASCE, Reston
 25. Pantoli E, Chen M, Wang X, Hutchinson T, Meacham B, Park H (2013) Shake table testing of a full-scale five-story building: seismic performance of the major nonstruc-

- tural components: egress systems, facades In: Proceedings, 2013 ASCE structures congress, ASCE, Reston
26. Meacham BJ, Kim JK, Park H (2013) Shake table testing of a full-scale five-story building: post-earthquake fire performance. In: Proceedings, 2013 structures congress, ASCE, Reston
 27. Park H, Meacham BJ, Kim JK (2014) Fire performance of full-scale building subjected to earthquake ground motion: fire test program and outcomes. In: Proceedings, 11th international symposium on fire safety science, international association for fire safety science. <http://www.iafss.org/publications/fss/11/71/view>
 28. Kim JK, Meacham BJ, Park H, Hutchinson T, Pantoli E (2014) Fire performance of full-scale building subjected to earthquake ground motion: test specimen, ground motions and seismic performance of fire protection systems. In: Proceedings, 11th international symposium on fire safety science, international association for fire safety science. <http://www.iafss.org/publications/fss/11/90/view>
 29. Wang X, Pantoli E, Hutchinson TC, Restrepo J, Wood RL, Hoehler MS, Grzesik P, Sesma FH (2015) Seismic performance of cold-formed steel wall systems in a full-scale building. *J Struct Eng*. doi:10.1061/(ASCE)ST.1943-541X.0001245
 30. Meacham BJ (2015) Towards a risk-informed performance-based approach for post-earthquake fire protection design of buildings. In: Proceedings, 10th Asia-Oceania symposium on fire science and technology, Tsukuba. 5–7 Oct 2015 (in press)
 31. LHPOST specifications. <http://nees.ucsd.edu/facilities/shake-table.shtml>. Accessed 20 April 2015
 32. Wang X, Ebrahimian H, Astroza R, Conte J, Restrepo J, Hutchinson T (2013) Shake table testing of a full-scale five-story building: pre-test simulation of the test building and development of a nonstructural components and systems design criteria. In: Proceedings, ASCE structures congress, ASCE, Pittsburgh
 33. Tian Y, Filiatrault A, Mosqueda G (2013) Experimental seismic study of pressurized fire sprinkler piping systems, Report MCEER-13-0001, p 404
 34. Soroushian S, Maragakis EM, Zaghi AE, Echevarria A, Tian Y, Filiatrault A (2014) Comprehensive analytical seismic fragility of fire sprinkler piping systems, Technical Report MCEER-14-02, August 26, 2014. <http://mceer.buffalo.edu/pdf/report/14-0002.pdf>
 35. Hokugo A, Kaneko T, Sekizawa A, Kakegawa S, Notake H (2011) A study on evacuation simulation after earthquake in consumer facilities. In: Peacock RD (ed) *et al* Pedestrian and evacuation dynamics Springer, Berlin, pp 793–797. doi:10.1007/978-1-4419-9725-8_76
 36. Porter KA, Kiremidjian AS, Le Grue JS (2001) Assembly-based vulnerability of buildings and its use in performance evaluation. *Earthq Spectra* 17(2):291–312. doi:10.1193/1.1586176
 37. Collier PCR (2005) Post-earthquake performance of passive fire protection systems, BRANZ
 38. Babrauskas V (2002) Heat release rate. In: DiNunno PJ (ed) *The SFPE handbook of fire protection engineering*, 3rd edn. National fire protection association, Quincy. p 3/25
 39. Kim J-K (2014) A conceptual framework for assessing post-earthquake fire performance of buildings, MS Thesis, Department of Fire Protection Engineering, Worcester Polytechnic Institute, Worcester
 40. ATC-58 (2012) Guidelines for seismic performance assessment of buildings (100% draft). Applied Technology Council, Redwood City
 41. SFPE (2000) SFPE engineering guide to performance—based fire protection analysis and design of buildings. SFPE, Bethesda

42. Reinhorn AM, Ryu KP, Maddaloni G (2010) Modeling and seismic evaluation of non-structural components: testing frame for experimental evaluation of suspended ceiling systems, Report MCEER-10-0004, June 2010, p 182
43. Davies R, Retamales R, Mosqueda G, Filiatrault A (2011) Experimental seismic evaluation, model parameterization and effects of cold-formed steel-framed gypsum partition walls on the seismic performance of an essential facility, Report MCEER-11-0005, October 2011, p 218. <http://mceer.buffalo.edu/pdf/report/11-0005.pdf>
44. PyroSim User Manual (2014) Thunderhead engineering. Manhattan. https://www.thunderheadeng.com/wp-content/uploads/dlm_uploads/2014/02/PyroSimManual.pdf
45. Fire dynamics simulator (Version 6)—user’s guide (2012) Gaithersburg. U.S. Department of Commerce, Technology Administration, National Institute of Standards and Technology
46. Pathfinder User Manual (2014) Thunderhead engineering. Manhattan. http://www.thunderheadeng.com/wp-content/uploads/downloads/2014/10/users_guide.pdf
47. Hokugo A, Kaneko T, Sekizawa A, Kakegawa S, Notake H (2011) Pedestrian and evacuation dynamics, A study on evacuation simulation after earthquake in consumer facilities. Springer, Berlin, pp. 793–797